

**The Effects of Nano-sized Hydroxyapatite on
Demineralization Resistance and Bonding Strength
in Light-Cured Glass Ionomer Dental Cement**

Ji Hee Kim

**The Graduate School
Yonsei University
Department of Dental Science**

**The Effects of Nano-sized Hydroxyapatite on
Demineralization Resistance and Bonding Strength
in Light-Cured Glass Ionomer Dental Cement**

A Dissertation Thesis

Submitted to the Department of Dental Science
and the Graduate School of Yonsei University

in partial fulfillment of the
requirements for the degree of
master of Dental Science

Ji Hee Kim

June 2008

This certifies that the dissertation
of Ji Hee Kim is approved.

Thesis Supervisor : Prof. Hyung Jun Choi

Byung Jai Choi

Yong Keun Lee

The Graduate School

Yonsei University

June 2008

감사의 글

본 논문의 연구 계획에서부터 완성에 이르기까지 자상하게 지도해주시고 격려를 아끼지 않으셨던 최형준 지도 교수님께 깊은 감사를 드리며 꼼꼼한 지적과 소상한 가르침을 베풀어 주셨던 최병재 교수님, 실험 설계와 진행에 있어서 지도와 조언을 아끼지 않으셨던 이용근 교수님께 진심으로 감사드립니다. 아울러 관심 있게 지켜봐 주신 손흥규 교수님, 이제호 교수님, 멀리 미국에 계신 김성오 교수님, 항상 가까이에서 아낌없는 관심과 조언을 해 주시는 송제선 임상교수님께도 감사드립니다. 또한 실험의 기술적인 부분을 세심하게 도와주신 치과재료학교실의 이병현 선생님을 비롯한 여러 선생님들께도 깊은 감사를 드립니다.

바쁜 병원 생활 속에서도 항상 깊은 관심을 보여주고 힘이 되어주는 이효설 선생님, 논문 작성 중 많은 도움을 준 김승혜 선생님, 확진회, 실험 과정 중 격려와 조언을 아끼지 않으신 이정진 선생님, 그리고 다른 소아치과 의국원들에게도 감사드립니다.

끝으로 헌신적인 사랑과 한결 같은 정성으로 돌보아 주시며 늘 저의 빈자를 채워주시는 사랑하는 부모님께 깊은 감사를 드리며, 변함 없는 사랑과 관심으로 항상 도움을 주는 대홍 오빠와 소영 언니에게도 깊은 감사의 뜻을 전하면서 이 조그만 결실을 함께 나누고자 합니다.

저자 씀

Table of contents

List of Figures.....	iii
List of Tables.....	iv
Abstract.....	v
I. Introduction.....	1
II. Materials and Methods.....	5
1. Materials.....	5
2. Methods	
A. Preparing the light-cured glass ionomer cement containing the hydroxyapatite.....	8
B. ISO test.....	9
(1) Depth of cure.....	9
(2) Sensitivity to ambient light.....	10
(3) Flexural strength.....	11
C. Acid demineralization test and surface observation by CLSM and SEM.....	12
D. Bonding strength and surface observation by SEM.....	14
E. Statistical analysis.....	16

III. Result

1. ISO test.....	17
A. Depth of cure.....	17
B. Sensitivity to ambient light.....	19
C. Flexural strength.....	20
2. Surface observation by CLSM after acid demineralization.....	22
3. Surface observation by SEM after acid demineralization.....	23
4. Bonding strength.....	26
5. Observation of fracture surfaces by SEM after measuring bonding strength.....	28
IV. Discussion.....	32
V. Conclusion.....	41
References.....	44
Abstract in Korean.....	50

List of Figures

Fig. 1. Fuji II LC GIC (GC Co., Japan).....	6
Fig. 2. EliparTM FreeLight (3M/ESPE, USA).....	6
Fig. 3. Calcium phosphate tribasic (Sigma-Aldrich Inc., USA).....	7
Fig. 4. Medical grade extra pure nano powder HA (OssGen Inc., Korea).....	7
Fig. 5. Sample for the investigation of bonding strength.....	15
Fig. 6. Depth of cure (mm).....	18
Fig. 7. Flexural strength (MPa).....	21
Fig. 8. Interface between tooth and cement under CLSM after acid demineralization (x 10).....	22
Fig. 9. SEM images of the sagittally sectioned enamel surface adjacent to the cement after acid demineralization.....	25
Fig. 10. Bonding strength (mN/mm²).....	27
Fig. 11. SEM images of fracture surface after measuring bonding strength (x 200).....	29
Fig. 12. SEM images of fracture surface after measuring bonding strength.....	31

List of Tables

Table 1. Sample identification of LC GIC.....	8
Table 2. Content's ingredients of acid buffer solution (pH 5.0).....	13
Table 3. The components of simulated body fluid (SBF).....	15
Table 4. Depth of cure (mm).....	18
Table 5. Flexural strength (MPa).....	21
Table 6. Bonding strength (mN/mm²).....	27

Abstract

The Effects of Nano-sized Hydroxyapatite on Demineralization Resistance and Bonding Strength in Light-Cured Glass Ionomer Dental Cement

Light-cured glass ionomer cement (LC GIC) was developed in the 1980s to reduce the setting time and to improve resistance to dehydration of conventional GIC while maintaining its properties – fluoride release over a prolonged period, specific adhesion to enamel and dentin, esthetics. Currently, LC GIC has a variety of clinical applications, as it has superior physical properties compared to conventional GIC and is more biocompatible than resin. However, it has certain limitations in that secondary dental caries may occur due to microleakage and that the restorations lack adequate retention. Therefore, increase in bonding strength and physical properties of LC GIC, while maintaining its biocompatibility, is needed.

Hydroxyapatites (HA) are the major components of dental enamel and bone mineral as biological apatites. In addition, HA contains a significant amount of calcium and phosphate, which can promote remineralization of enamel subsurface lesions in animals and humans. Recently, researchers in the field of dentistry have utilized nanotechnology to make nano-sized HA particles. These

nano HA particles can be added to a LC GIC, imparting demineralization resistance and promoting remineralization of the enamel surface.

The aim of this study was to evaluate the effect of incorporated nano HA on the demineralization resistance and bonding strength of LC GIC in comparison with micro HA.

Fuji II LC GIC (GC Co., Japan) was used as the control group and a base material for experimental groups. Two experimental groups were prepared. One was prepared by adding 15% nano HA to LC GIC by weight ratio, and the other was prepared by adding 15% micro HA instead.

The depth of cure, sensitivity to ambient light, and flexural strength, which are the necessary requirements for dental water-based light activated cements, were determined according to ISO 9917-2:1998. And in order to observe the demineralization resistant effect of each material, sectioned specimens were observed under CLSM and SEM after 4 days of demineralization. Four weeks after the assembly of tooth-cement had been immersed in SBF at 37°C, the shear bonding strength was measured and the fractured surface of the specimen was observed under SEM. According to the results, the following conclusions could be obtained.

1. The depth of cure was found to be in the decreasing order of pure Fuji II LC GIC, 15% micro HA-Fuji II LC GIC, 15% nano HA-Fuji II LC GIC group, and there were statistically significant differences between the three groups ($p < 0.05$). The curing depth in all groups satisfied the required curing depth of ISO 9917-2:1998 (minimum curing depth = 1 mm).
2. Regarding the sensitivity to ambient light, there were no detectable changes in the homogeneity in any group.
3. The flexural strength was found to be in the increasing order of 15% nano HA-Fuji II LC GIC, pure Fuji II LC GIC, 15% micro HA-Fuji II LC GIC group, and there were statistically significant differences between the three groups ($p < 0.05$). All groups satisfied the required flexural strength of ISO 9917-2:1998 (minimum flexural strength = 20 MPa).
4. Observing under the CLSM after 4 days of acid demineralization, the control group showed thicker enamel demineralization layer than in the experimental groups, and the 15% nano HA-Fuji II LC GIC group showed the thinnest demineralization layer.
5. In SEM analysis, there was greater enamel demineralization in the control group. As less demineralized occurred under the influence of HA

particles, the experimental groups revealed relatively even surface particles. Comparing the two experimental groups, the 15% nano HA-Fuji II LC GIC group was more resistant to demineralization compared to the 15% micro HA-Fuji II LC GIC group.

6. The bonding strength was found to be in the increasing order of pure Fuji II LC GIC, 15% micro HA-Fuji II LC GIC, 15% nano HA-Fuji II LC GIC group, and there were statistically significant differences between the three groups ($p < 0.05$).
7. Observing the fractured surfaces under SEM after the bonding strength test was performed, the cohesive failure ratio was found to be in the increasing order of pure Fuji II LC GIC, 15% micro HA-Fuji II LC GIC, 15% nano HA-Fuji II LC GIC group. There were bone-like apatite particles formed in HA-added experimental groups, and a greater number of bone-like apatite particles were formed in the 15% nano HA-Fuji II LC GIC group compared to the 15% micro HA-Fuji II LC GIC group.

15% micro HA and 15% nano HA were used in this study, and we found that although the addition of nano HA to LC GIC resulted inferior flexural strength compared to the addition of micro HA, nano HA lead to superior

demineralization resistance as well as superior bonding strength. Assuming similar results can be achieved in the oral environment, clinicians can prevent demineralization of enamel surface by using nano HA. Further study is needed to determine the optimal concentration for proper physical properties of the cement.

**Key words : light-cured glassionomer cement, nano-sized hydroxyapatite,
demineralization resistance, bonding strength**

The Effects of Nano-sized Hydroxyapatite on Demineralization Resistance and Bonding Strength in Light-Cured Glass Ionomer Dental Cement

Ji Hee Kim

Department of Dental Science, The Graduate School Yonsei University

<Directed by professor Hyung Jun Choi, DDS, PhD>

I. Introduction

A particular category of bioactive materials represented by the glass ionomer cement (GIC) has been recommended for a wide range of clinical applications. This popularity is due to the fact that GIC presents several important properties expected from an ideal restorative material, such as fluoride release (Gao W and Smales RJ, 2001), coefficient of thermal expansion and modulus of elasticity similar to that of dentin (Bullard RH et al., 1998), chemical bonding to both enamel and dentin (Erickson RL and Glasspoole EA, 1994), and biocompatibility (Leyhausen G et al., 1998; Costa CAS et al., 2003). In the clinic, however, the use

of GIC is limited due to its susceptibility to dehydration (Cho E et al., 1995) and poor physical properties, such as high solubility and slow setting rate (Mount GJ, 1999). Light-cured glass ionomer cement (LC GIC) was developed in the 1980s to reduce the setting time and to improve resistance to dehydration of conventional GIC while maintaining its properties – fluoride release over a prolonged period, specific adhesion to enamel and dentin, esthetics. Currently, LC GIC has a variety of clinical applications, as it has superior physical properties compared to conventional GIC and is more biocompatible than resin. However, it has certain limitations in that secondary dental caries may occur due to microleakage and that the restorations lack adequate retention. Therefore, increase in bonding strength and physical properties of LC GIC, while maintaining its biocompatibility, is needed.

Recently there are many studies being conducted to see the effect of the addition of hydroxyapatite (HA) to various dental materials in an attempt to improve the physical properties. The use of HA in restorative dentistry offers several promising advantages, including its biocompatibility, intrinsic radiopaque response, enhanced polishability, and improved wear performance, because synthetic HA has a hardness similar to that of natural teeth. In addition, HA contains a significant amount of calcium and phosphate, which can promote remineralization (Anderson P et al., 2004). The incorporation of HA into dental restorative materials, such as resin or GIC, has been found to enhance flexural

strength and Young's modulus (Santos C. et al., 2001), compressive strength, and bonding strength (Yoon SI et al., 2005). It has also been reported that HA incorporation into chewing gums, toothpastes, mouthrinse improves enamel remineralization (Itthagarum A et al., 2005; Jeong SH et al., 2006; Kuilong LV. et al., 2007). The remineralization effect of HA may be because HA can act as a mineral reservoir, which dissociates to form calcium, phosphate ions and hydroxyl ions and fill the micro-sized fine pores of the demineralized enamel surfaces. However, because the micropores between enamel prisms are about 0.1 μm wide, it was hard to expect the conventional 0.2~0.3 μm HA to directly fill up the micropores on demineralized enamel surfaces.

Together with biotechnology, the recent emergence of the new, nanotechnology, is spotlighted as the core technology to lead the new 21 century industrial businesses. Through nanotechnology, it is now possible to convert micrometer particles into nano-sized particles and produce new physical properties from the exact same material and chemical compositions of conventional restorations (Jeong SH et al., 2006; Kim BI et al., 2006). The HA particles on enamel surface have an average size of 100 μm , which is fairly large compared to those in bone tissue or dentin (Kloke A, 2003). The particles are also well aligned, paralleled to each other. But because the enamel does not include collagen-like organic materials as does the bone tissue and dentin (Lowenstam HA, 1989), however, it is necessary to consider the conventional bonding strength to enamel when

developing artificial HA. Compared to the previously widely used micro-sized synthetic HA, the greatly minimized nano-sized particles of the nano HA have greater surface areas (Arcis RW et al., 2002) and solubility (Domingo C et al., 2001) that they are expected to be outstanding in filling micropores of demineralized enamel surfaces, and also in providing inorganic ions such as calcium and phosphate (Huang M et al., 2003), thus increasing the bonding strength to the tooth. Recent studies have shown that the addition of nano HA to conventional GIC improved bonding strength and demineralization resistance, but so far there has been no study regarding the effects of adding nano HA to LC GIC. The aim of this study was to evaluate the effect of incorporated nano HA on the demineralization resistance, and bonding strength of LC GIC in comparison with micro HA.

II. Materials and Methods

1. Materials

We prepared commercially available LC GIC and HA of two different particle sizes (micro-sized HA, nano-sized HA). Fuji II LC (GC Co., Japan) was used as the control group and a base material for experimental groups (Fig. 1) and EliparTM FreeLight (3M/ESPE, USA) was used as a light curing source (Fig. 2).

Calcium phosphate tribasic (Sigma-Aldrich Inc., USA)(Fig. 3) was the micro-sized HA powder of choice. Its molecular formula is $\text{Ca}_5(\text{OH})(\text{PO}_4)_3$ and its particle diameter about 5~10 μm .

Medical grade extra pure nano powder hydroxyapatite (OssGen Inc., Korea)(Fig. 4) was selected to represent HA with nano-particles, and the molecular equation of the materials is $\text{Ca}_{10}(\text{PO}_4)_6(\text{OH})_2$, and the average particle size 100~150 nm.



Fig. 1. Fuji II LC GIC (GC Co., Japan).



Fig. 2. EliparTM FreeLight (3M/ESPE, USA).

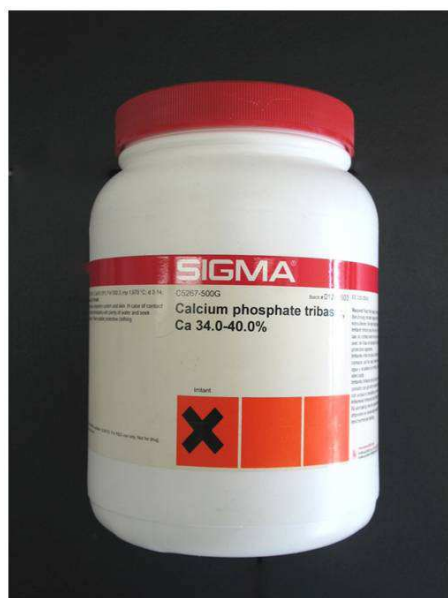


Fig. 3. Calcium phosphate tribasic (Sigma-Aldrich Inc., USA).



Fig. 4. Medical grade extra pure nano powder HA (OssGen Inc., Korea).

2. Methods

A. Preparing of HA-LC GIC

In that 15% micro HA-Fuji II LC GIC has presented the best physical characters in previous studies, 15% micro HA-Fuji II LC GIC and 15% nano HA-Fuji II LC GIC were used.

15% mixture ratio was measured by weight ratio, and in order to acquire even mixtures, Ball mill (Samwoo Scientific Co., Korea) was used under 400 rpm for 24 hours.

The recommended powder-liquid ratio was 2 for Fuji II LC GIC.

Fuji II LC GIC was used in the control group and the experimental groups were 15% micro HA-Fuji II LC GIC and 15% nano HA-Fuji II LC GIC (Table 1).

Table 1. Sample identification of LC GIC

Sample I. D.	LC GIC	wt% of HA
LC GIC (Control 1)	Fuji II	0
Micro HA-LC GIC (Exp. 1)	Fuji II	15
Nano HA-LC GIC (Exp. 2)	Fuji II	15

B. ISO test

The depth of cure, sensitivity to ambient light, and flexural strength, which are the necessary requirements for dental water-based light activated cements, were determined under regulations of ISO 9917-2:1998. They were tested using Fuji II LC GIC, 15% micro HA-Fuji II LC GIC and 15% nano HA-Fuji II LC GIC, maintaining the constant liquid powder ratio.

(1) Depth of cure

LC GIC was condensed into a mold (6mm long and 4mm in diameter) and was then pressed between two matrix strips and two glass plates. The glass plate covering top of the mold was removed and the exit window of light curing unit was gently placed on the matrix strip covering the mold. The LC GIC was then cured for 20 seconds as recommended by the manufacturer. After curing, the specimen was immediately removed from the mold, and the uncured portion was gently removed with a knife. The height of cured portion was measured in micrometers and was divided by two.

(2) Sensitivity to ambient light

Thirty milligrams of LC GIC was placed as a spheroid mass on a glass slide and was exposed to a Xenon lamp for 30 seconds to provide an illuminance of 8,000 lux. The glass slide was then removed from the illuminated area and a second microscope slide was immediately pressed against the material with a slight shear action to produce a thin layer. LC GIC was visually inspected to see whether it was homogenous with no discernible voids or defects. The whole procedure was repeated twice using new samples of LC GIC for each test.

(3) Flexural strength

Specimens with a dimension of 25 x 2 x 2 mm were prepared using stainless-steel split molds. Materials were packed into the mold placed on a polyester film. A second polyester film was placed on the material and was covered with a glass plate. Pressure was applied to cause excess material to extrude. The light curing unit was then placed at the center of the specimen and irradiated for 20 seconds. After curing, the assembly was placed in the water bath of 37°C for 24 hours. Then, a load was applied onto the specimen with crosshead speed of 0.75 mm/min using a universal testing machine (Instron, UK) until the specimen fractured. The applied load was recorded at the moment of specimen fracture, and the flexural strength (σ) was calculated in MPa using the following equation.

$$\sigma = 3FI/2bh^2$$

F = the maximum load applied (N)

I = the distance between the supports (mm)

b = width of the specimen (mm)

h = height of the specimen (mm)

C. Acid demineralization test and surface observation by CLSM and SEM

Box-shaped cavities (6mm x 2mm x 1.5mm) were prepared along the cemento-enamel junction of human molars. The cavity margins were finished with a slow-speed fissure bur, giving a cavo-surface angle as close to 90°. The cavities were then filled with LC GIC, which was irradiated for 20 seconds with the light curing unit. The cavities were slightly overfilled to compensate the curing shrinkage of cement, and they were polished using Sof-LexTM disk after curing.

Two coats of an acid-resistant varnish were then applied to the tooth surface, leaving a 1 mm window without varnish around the cavity margins. The teeth were then placed in 25 ml of acid buffer solution containing 2.2 mM CaCl₂, 2.2 mM NaH₂PO₄, and 50 mM acetic acid for 4 days at 37°C (Table 2). The acid solution was replaced every 24 hours.

After 4 days, the teeth were embedded into cylindrical epoxy-resin to be made into slide specimens. By using an EXAKT diamond band saw (EXAKT Co., Germany), the teeth were sawed parallel to the long axis, passing through the center of the restoration material. The sectioned surface of specimens was observed under a confocal laser scanning microscope (CLSM) (LSM 510, Carl Zeiss Meditec AG, Germany) and a scanning electron microscope (SEM) (S 2000, Hitachi, Japan) to examine the demineralization patterns of enamel adjacent to

the cement material.

For microscopic observation under CLSM examination, the samples were dyed in 0.1 mM rhodamine B solution for 1 hour, washed with distilled water and dried. The CLSM causes the demineralized lesions on the enamel to fluoresce under the He-Ne laser light, which has a 543 nm excitation wavelength and a 560 nm long-pass barrier filter.

Table 2. Content's ingredients of acid buffer solution (pH 5.0)

Materials	Molecular weight	Vol.	Weight	Concent
	(g/mol)	(ml)	(g)	(M)
CaCl ₂	110.98	1500	0.3662472	2.2 mM
NaH ₂ PO ₄ ·2H ₂ O	156.01	1500	0.51	2.2 mM
CH ₃ COOH	60.05	1500	4.503942	50 mM

D. Bonding strength and surface observation by SEM

In order to measure the bonding strength, a total of 15 extracted permanent molars, 5 from each group, were used. Teeth were embedded into cylindrical epoxy-resin molds (25 mm x 25 mm x 25 mm), with the intended site for bonding facing the bottom of the mold. The embedded specimens were ground flat perpendicular to the long axis of each tooth until the exposed enamel or dentin surface was large enough to bond a cylinder of restorative material (Fig. 5, a). The exposed surface was then etched with 35% phosphoric acid, removing the smear layer. Next, each cylindrical mold (6 mm in diameter, 6 mm in height) was placed on the etched tooth surface and the material was poured into the mold. The cylindrical specimens were attached to the tooth surface by light curing for 20 seconds (Fig. 5, b). Afterwards, each sample was kept under pH 7.4 simulated body fluid (SBF) (Table 3), at 37°C, and the fluid was changed every week. After four weeks, the cylindrical specimens were loaded by a metal rod on a universal testing machine (Instron, UK) in a direction perpendicular to the long axis at 1 mm/min until fracture occurred. The shear bonding strength was calculated as a ratio of fracture load over bonding area, and was expressed in mN/mm^2 .

After measuring the shear bonding strength, the fractured surfaces of the specimens were observed under various magnifications using SEM (Hitachi S-800, Japan).

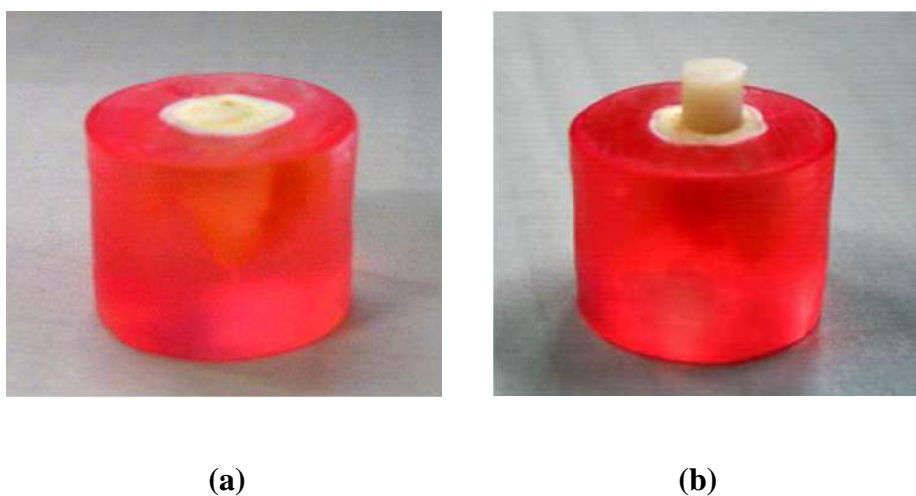


Fig. 5. Sample for the investigation of bonding strength.

Table 3. The components of simulated body fluid(SBF) in this study

List	Material	1L (g)	500ml (g)
1	NaCl	7.996	3.998
2	NaHCO ₃	0.35	0.175
3	KCl	0.224	0.112
4	K ₂ HPO ₄ .3H ₂ O	0.174	0.087
5	MgCl ₂ .6H ₂ O	0.305	0.1525
6	1M-HCl	40 ml	20
7	CaCl ₂	0.278	0.139
8	Na ₂ SO ₄	0.071	0.0355
9	NH ₂ C(CH ₂ OH) ₃	6.057	3.0285

E. Statistical analysis

Statistic analysis was done on SAS 8.2 version. In order to examine the differences in depth of cure, flexural strength and bonding strength between the control, experimental groups, the Kruskal-Wallis test was used (p value = 0.05). A post-hoc test was then carried out through the Dunn procedure, in order to verify the groups that showed differences. Each test result was presented as the median and the range.

III. Results

1. ISO test

A. Depth of cure

Compared to 4.72 mm depth of cure of the control group, both experimental groups showed smaller depth of cure; 4.35 mm in the Exp. 1 group and 3.01 mm in the Exp. 2 group (Table 4, Fig. 6).

Through the Kruskal-Wallis test, significant differences were found between the three groups ($p < 0.05$). Through the post-hoc test using the Dunn procedure, significant differences were found between the control group and the Exp. 2 group (critical value = 2.393).

All groups satisfied the ISO requirement for the minimum curing depth of 1 mm.

Table 4. Depth of cure (mm)

	Control	Exp. 1	Exp. 2
Median	4.720*	4.350	3.010*
Range	4.530~4.870	4.210~4.410	2.930~3.120

* : Statistically significant at critical value = 2.393 by Dunn procedure

(minimum curing depth = 1 mm)

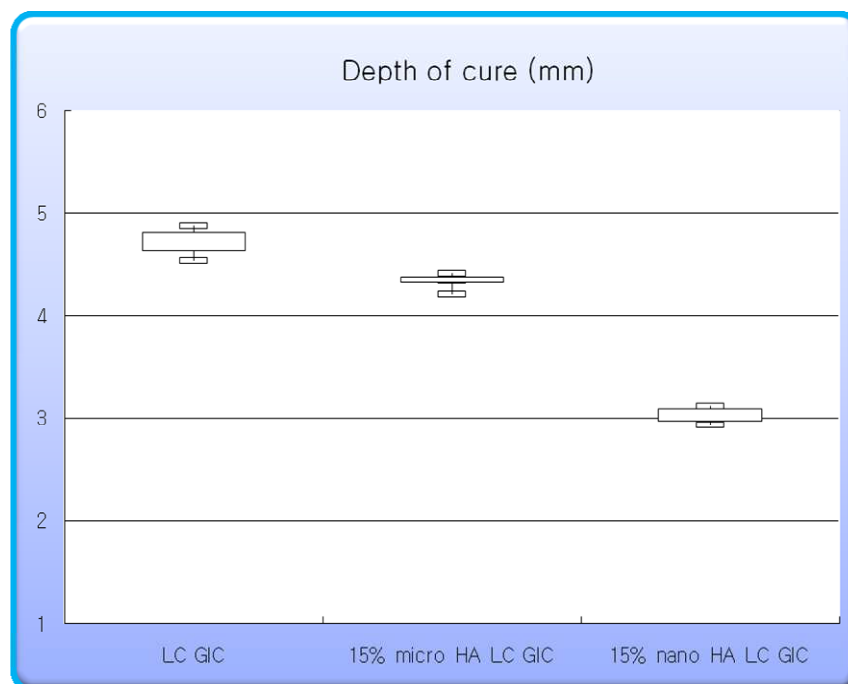


Fig. 6. Depth of cure (mm)

B. Sensitivity to ambient light

In all groups, homogeneity was maintained after the completion of the test, showing no clefts or voids. Sensitivity to ambient light, therefore, was not observed in any group.

C. Flexural strength

The Exp. 1 group showed 84.086 MPa of flexural strength that is greater than 70.082 MPa of the control group, whereas the Exp. 2 group showed a smaller flexural strength of 58.680 MPa (Table 5, Fig. 7).

Through the Kruskal-Wallis test, significant differences were found between the three groups ($p < 0.05$). Through the post-hoc test using the Dunn procedure, significant differences were found between the Exp. 1 group and the Exp. 2 group (critical value = 2.393).

All groups satisfied the ISO requirement for the minimum flexural strength of 20 MPa.

Table 5. Flexural strength (MPa)

	Control	Exp. 1	Exp. 2
Median	70.082	84.086*	58.680*
Range	59.826 ~ 73.648	76.989 ~ 112.769	50.089 ~ 62.876

* : Statistically significant at critical value = 2.395 by Dunn procedure

(minimum flexural strength = 20 MPa)

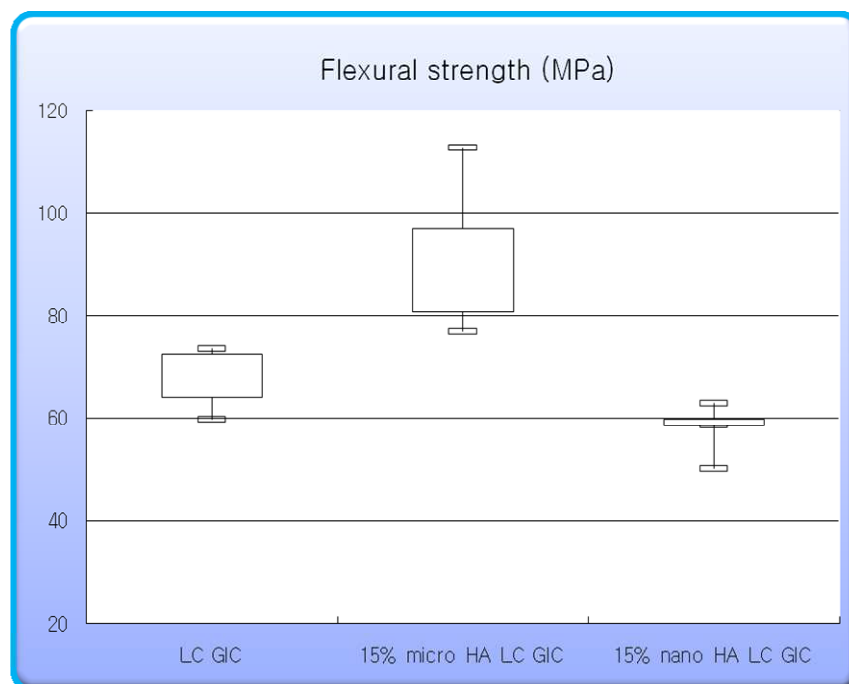


Fig. 7. Flexural strength (MPa)

2. Surface observation by CLSM after acid demineralization

CLSM allows the demineralized surface layers of enamel to be visualized down to approximately 100 μ m. The control group had a relatively thick fluorescent layer compared to the two experimental groups.

Comparing the two experimental groups, the Exp. 2 group had the thinnest fluorescent layer (Fig.8).

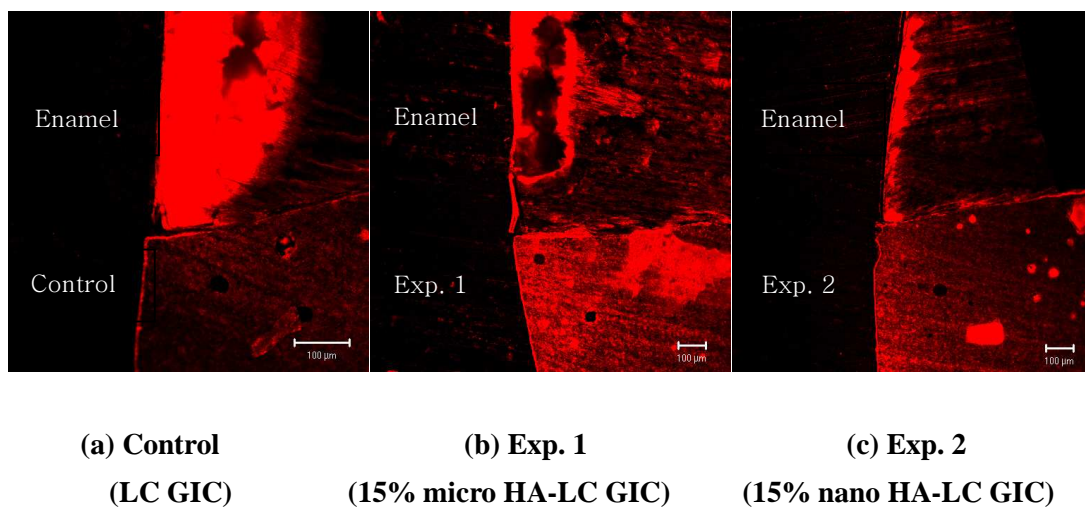
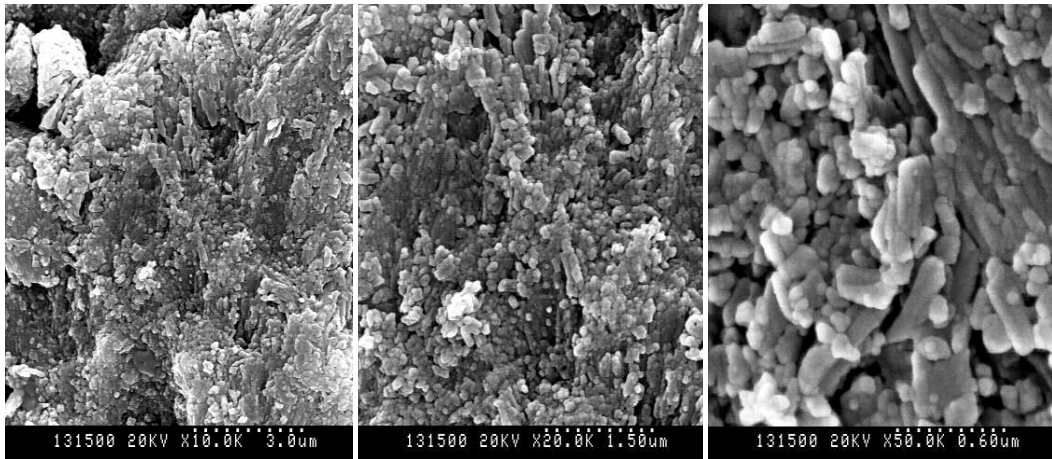


Fig. 8. Interface between tooth and cement observed under CLSM after acid demineralization (x 10).

3. Surface observation by SEM after acid demineralization

The SEM images of micro surfaces demonstrated small morphological differences between the control group and the experimental groups (Fig. 9). The control group showed more irregular granular and porous surfaces than the experimental groups after acid demineralization. Comparing the two experimental groups, there was less demineralization occurred in the Exp. 2 group, and thus less irregular and porous surfaces were created in the Exp. 2 group.

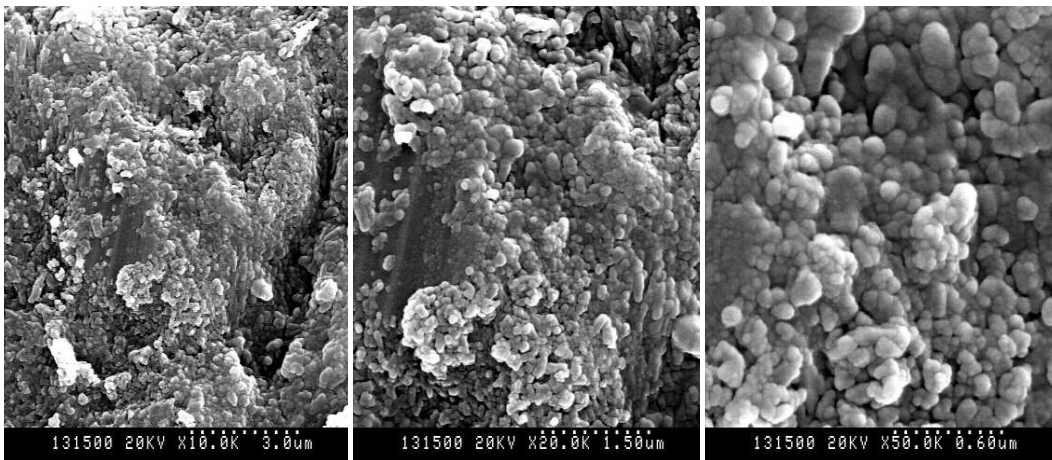


(X 10000)

(X 20000)

(X 50000)

(a) Control (LC GIC)

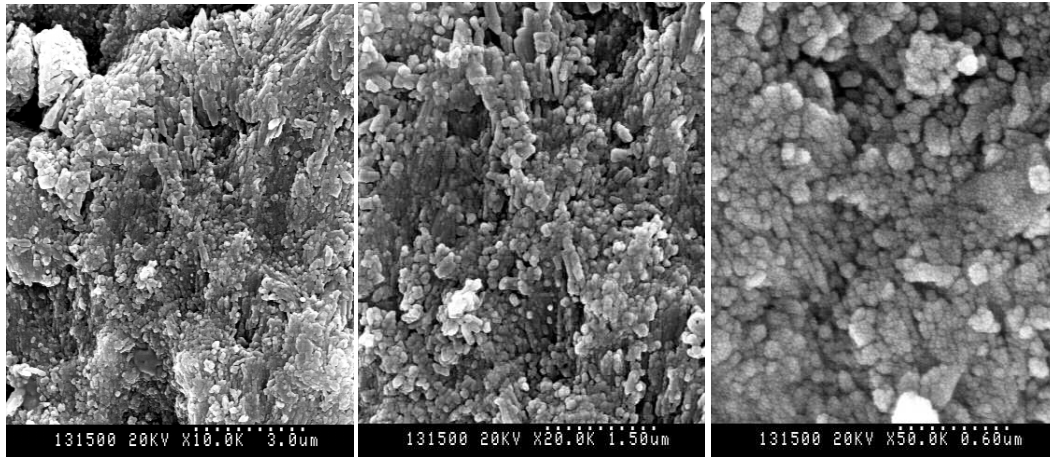


(X 10000)

(X 20000)

(X 50000)

(b) Exp. 1 (15% micro HA-LC GIC)



(X 10000)

(X 20000)

(X 50000)

(C) Exp. 2 (15% nano HA-LC GIC)

Fig. 9. SEM images of the sagittally sectioned enamel surface adjacent to the cement after acid demineralization.

The control group (a) showed greater irregularity and porosity on the enamel surface compared to the Exp. 1 group (b) or the Exp. 2 group (c). The Exp. 2 group (c) showed the least irregularity and porosity after acid demineralization.

4. Bonding strength

The bonding strength of cement to dentin increased to 419.20 mN/mm² in the control group, 1075.60 mN/mm² in the Exp. 1 group, 1911.50 mN/mm² in the Exp. 2 group (Table 6, Fig. 10).

Through the Kruskal-Wallis test, significant differences were found between the three groups ($p < 0.05$). Through the post-hoc test using the Dunn procedure, significant differences were found between the control group and the Exp. 2 group.

Table 6. Bonding strength (mN/mm²)

	Control	Exp. 1	Exp. 2
Median	419.20*	1075.60	1911.50*
Range	329.60 ~ 445.30	989.70 ~ 1217.20	1816.90 ~ 2002.50

* : Statistically significant at critical value = 2.395 by Dunn procedure

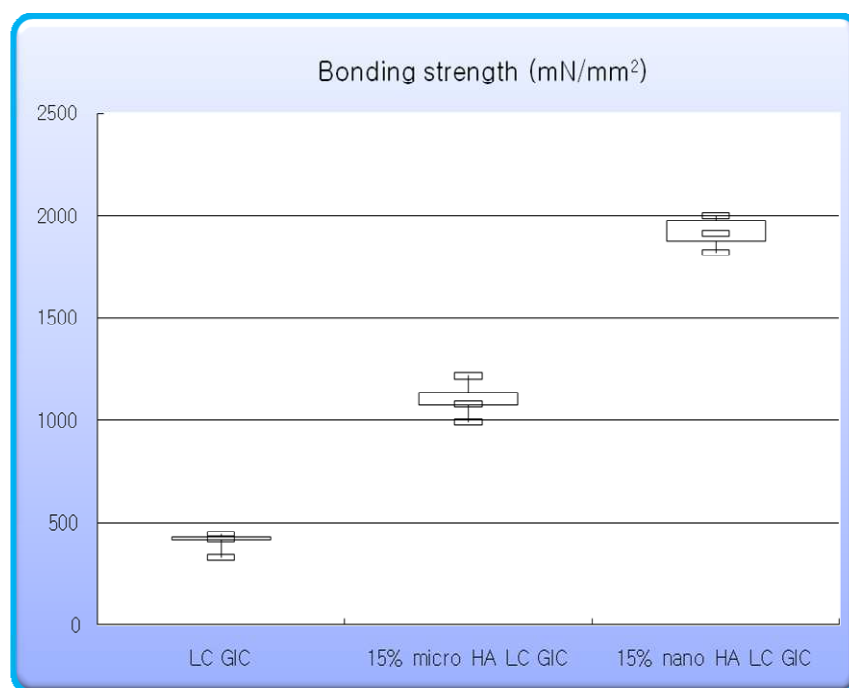


Fig. 10. Bonding strength (mN/mm²)

5. Observation of fracture surfaces by SEM after measuring bonding strength

When the fractured surfaces were observed under SEM at low magnification after the bonding strength test, the cohesive failure ratio increased in following order: the control group, the Exp. 1 group, and the Exp. 2 group (Fig. 11).

At higher magnifications the dentinal surfaces were fairly flat in the control group, but there were bone-like apatite particles formed in the experimental groups. A greater number of bone-like apatite particles were formed in the Exp. 2 compared to the Exp. 1 group (Fig. 12).

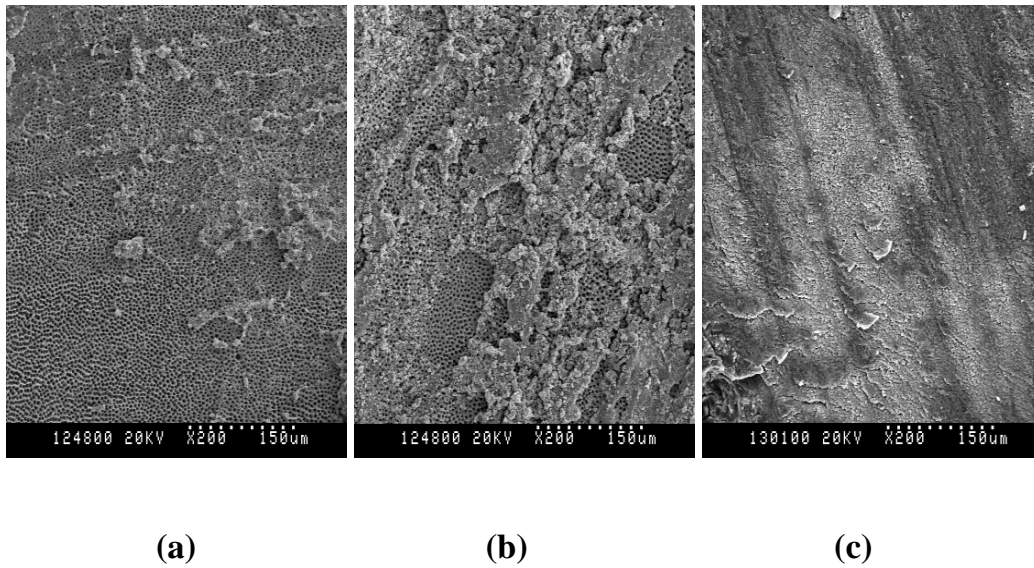
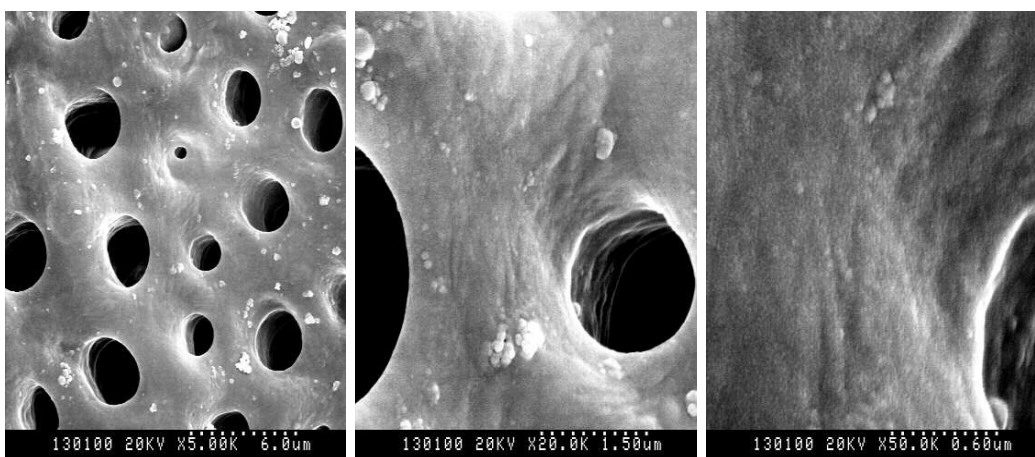


Fig. 11. SEM images of fracture surface after measuring bonding strength (x 200).

Increased appearance of cohesive failure was observed in the experimental groups (b, c) compared to the control group (a). The Exp. 2 group (c) had greater cohesive failure compared to the Exp. 1 group (b).

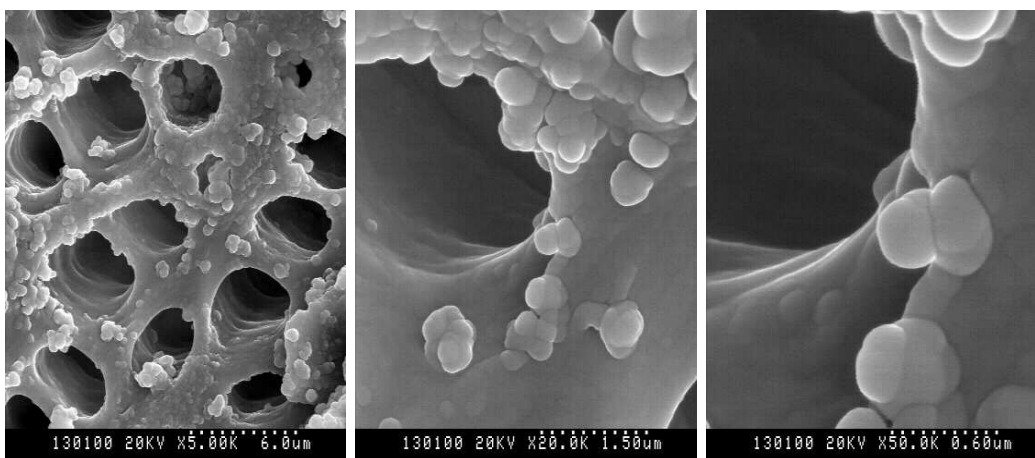


(X 5000)

(X 20000)

(X 50000)

(a) Control (LC GIC)

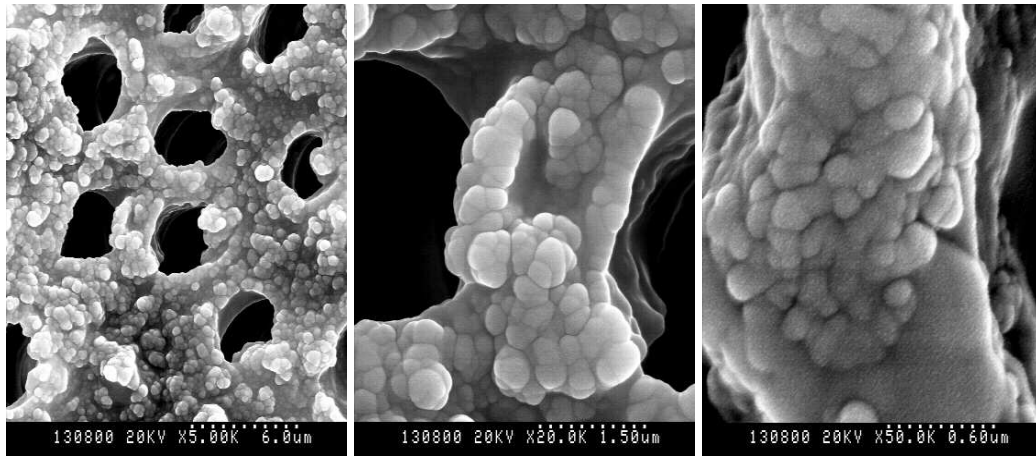


(X 5000)

(X 20000)

(X 50000)

(b) Exp. 1 (15% micro HA-LC GIC)



(X 5000)

(X 20000)

(X 50000)

(c) Exp. 2 (15% nano HA-LC GIC)

Fig. 12. SEM images of fracture surface after measuring bonding strength.

- (a) Control group, no bone-like apatite particles were observed on the tooth surface.
- (b) Exp. 1 group, the expected particles of bone-like apatite were formed on the tooth surface.
- (c) Exp. 2 group, the expected particles of bone-like apatite were formed on the tooth surface more than Exp. 1 group (b).

IV. Discussion

Hydroxyapatites (HA) are the major components of dental enamel and bone mineral as biological apatites. HA contains a significant amount of calcium and phosphate, which can promote remineralization of enamel subsurface lesions in animals and humans. Up to now, many researchers have confirmed that the biocompatibility of HA contribute to the enhancement of mechanical properties of various dental materials.

There are many studies conducted to apply nanotechnology to dental materials in the recent dental field. Because nano HA have greater surface areas and solubility compared to the micro HA, it is expected to show superior properties in filling micropores on demineralized enamel surfaces and in providing such inorganic ions as calcium and phosphate. In recent studies, nano HA, when added to the conventional glass ionomer cement (GIC), was found to enhance protection against acid demineralization of enamel surface and to increase the bonding strength to human teeth by forming bone-like apatites. But when nano HA was added to conventional GIC, however, its setting time exceeded the maximum setting time regulated by ISO 9917-1:2003(E). For actual clinical application, therefore, additional studies are needed to be done. Furthermore the use of GIC in clinics is limited due to its relatively weak mechanical properties and its sensitivity to initial desiccation and moisture (Mount GJ, 1999). Currently, light-

cured glass ionomer cement (LC GIC) has a variety of clinical applications as it has superior physical properties to conventional GIC, and is more biocompatible than resin. In this study, we attempted to compare the physical properties, the demineralization resistance and the bonding strength of not only the micro HA added to LC GIC, but also the nano HA, produced by the recently spotlighted nanotechnology.

Fuji II LC GIC (GC Co., Japan), used in this study, is a dental water-based light-activated cement. Fuji II LC GIC was used in the control group and the experimental groups used were 15% micro HA-Fuji II LC GIC and 15% nano HA-Fuji II LC GIC. To evaluate their suitability as dental cements, their curing depth, sensitivity to ambient light and flexural strength were assessed according to ISO 9917-2:1998 regulations. The control, Exp. 1, and Exp. 2 group showed the depth of cure in the decreasing order, and there were statistically significant differences between the three groups ($p < 0.05$). This may be due to the light-scattering effect of HA particles (Arcis RW et al., 2002).

Sensitivity to ambient light is a necessary parameter for light-activated materials, as ambient light may cause premature curing and result in crack and void formations during their use. There were no detectable changes in the homogeneity of any group after being exposed to the test light for 30 seconds, indicating that sensitivity to ambient light was not observed in any group.

Flexural strength gives an indication of the durability of restorative materials

and it is considered to be the most appropriate and reliable estimate of the strength of LC GIC (Gladys S et al., 1997). This study measured the flexural strength of the materials using a three-point flexural strength method. Flexural strength was measured to be greater in the Exp. 1 group than in the control group, and was smaller in the Exp. 2 group than in the control group. There were statistically significant differences between the three groups ($p < 0.05$). Number of reasons for the Exp. 1 group to present a greater flexural strength than the control group could be speculated. The increase in the flexural strength after the addition of HA is thought to be dependent primarily on a chemical reaction between the HA, glass powder and polyacid. Although the exact underlying chemical mechanism is yet unknown and requires further investigations, it is known to involve calcium ions from the HA. Since the glass used in commercial GIC are all alluminosilicate type containing calcium and fluoride ions, and react with polyacrylic acid to form ionic bonds, the addition of HA may provide extra calcium ions and facilitate the initial reaction. A previous study advocated that HA addition also facilitates increase in initial flexural strength of GIC in an aqueous storage condition (Lucas ME, 2002).

In LC GIC, when the polyacid reacts with the glass powder, it selectively binds to calcium ions first and then reacts with other ions. Therefore, when HA is added, the number of calcium ions in the initial reaction increase and thus the initial ionic bonds increase. Since the bonding between polyacrylic acid and glass ions

is the main reaction in LC GIC, the increase of flexural strength could be explained this way.

The size difference between the HA and GIC particles may also contribute to the increase of flexural strength, for the smaller particled HA may flow into the ionomer matrix of the bigger particled HA and induce a “packing effect” (Lucas ME et al., 2003, Gu YW et al., 2005).

As the reason for the Exp. 2 group to show weaker flexural strength than the control group, we may consider the increased solubility of nano HA (Domigo C et al., 2001). In case of nano particles, the “packing effect” induced by flowing into the ionomer matrix would obviously be greater than the micro particles, thus would increase the light scattering effect of the HA and decrease its flexural strength. This seems logical, observing the flexural strength increase as the density of HA increase and begin to decrease back at a certain point, while the density continue to increase (Glasspoole EA et al., 2002). The increase in HA content delays the polymerization of LC GIC, which in turn decreases the role of light polymerization while increasing that of autopolymerization. LC GIC was originally developed in 1986 by Autonucci to replace part of the water content of the glass ionomer system with a water-soluble monomer system that is polymerized by ambient free radical polymerization (Mckinney IE, 1986). LC GIC, thus, has a dual-setting mechanism involving acid-base reaction between polyacid and glass, simultaneously with polymerization reaction. Therefore any

portion of the material not cured by light may eventually be polymerized by autopolymerization. A previous study have reported a decrease in material strength cured by autopolymerization than cured by light polymerization (Glasspoole EA et al., 2002). Likewise, if the light-scattering effect of HA hinder light polymerization and shift the dual-setting reaction towards autopolymerization, a decrease in the material strength may eventually result.

In order to observe the demineralization resistant effect of each material, we kept the teeth in a pH 5.0 acid buffer solution for 4 days and cut them into slide specimens using a EXAKT diamond band saw. Under CLSM, the control, Exp. 1, and Exp. 2 group showed demineralization of the enamel in the decreasing order. From this, the assumption that demineralization resistance may increase with the addition of nano HA was confirmed. The demineralization observed under CLSM was found to be subsurface demineralization rather than enamel surface demineralization. This may be from the “coupled diffusion” resulting from the influx of acid and outflux of the dissolved materials (Anderson P, 2004).

Observing under SEM, the enamel surface of the control group was more uneven and showed greater loss of inorganic material between the enamel prisms than the HA-added experimental groups. Because the nano particles filled up the micropores formed by the loss of inorganic materials, the enamel surface of the Exp. 2 group was more smooth and even than that of the Exp. 1 group.

The reasons for increased demineralization resistance of nano HA are

considered to be the effect of direct filling of micropores on the demineralized enamel surface by the smaller size particles, and the effect of dissolving and providing the main inorganic components of HA, calcium and phosphate, with the high solubility (Huang M et al., 2003 ; Mazzaoui SA et al., 2003). Since the micropores between the enamel prisms are about 0.1 μ m, it was hard to expect it to be directly filled up by the 5~10 μ m micro HA, but the nano HA with an average size of 100~150nm showed an outstanding performance in doing so. The nano particles embedded into the micropores are also expected to impede the movement of calcium soaring from the enamel surface by the means of balancing the inorganic ions (Kim BI et al., 2006).

The control, Exp. 1, and Exp. 2 group presented the bonding strength in the increasing order, and there were statistically significant differences ($p < 0.05$). LC GIC is known for its ability to chemically bond to the tooth substrate, but the exact mechanism of chemical bonding of LC GIC to dental structures is not completely known. The probable mechanism of adhesion is based upon both diffusion and adsorption phenomena. The polyalkenoic acid of the glass ionomer will penetrate the tooth structure, releasing phosphate ions, each of which will take with it a calcium ion from the tooth surface to maintain electrical neutrality. These ions will combine with surface layer of cement and form an intermediate layer of a new material, which is firmly attached to the tooth surface (Geiger SB and Weiner S, 1993). This has been described as a “diffusion based adhesion”

(Akinmade AO and Nicholson JW, 1993). There is also a degree of adhesion available to the collagen of dentin through either hydrogen bonding or metallic ion bridging between the carboxyl groups on the polyacid and the collagen molecules (Akinmade A, 1994). The reason for increased bonding strength by adding HA, one of the main components of the tooth, to LC GIC that chemically bonds to tooth surface, was considered to be from the participation of calcium ions from the HA in the chemical bonding of the tooth and the material (Lucas ME et al., 2003). The bonding strength was greater in the Exp. 2 than in the Exp. 1 group, in that smaller particles make the surface areas greater, and the adhesion rate of the particles to the surface greater that they invade into the enamel surface and between the micropores and eventually provide greater bonding strength. Additional insight into this field was contributed by recent X-ray photoelectron spectroscopy studies (Sennou HE et al., 1999). Sennou have shown the formation of an intermediate dentin-glass ionomer layer on the surface of the materials that enables the exchange of mineral and organic elements and consequently the adhesion of the material to dentin.

In the SEM observation of the fractured surfaces, the most common mode of adhesion failure between the LC GIC and the dentin appeared during the bonding strength tests, was cohesive failure within the LC GIC. This result is in accord with the study done by Ngo et al (1997) that advocated the bonding strength between the hard tissue of the tooth and the cement matrix is stronger than the

strength between the cement matrix and glass particles. It is known that the pores in a solid body act as stress-concentration points where fracture can initiate (Griffith AA, 1920), and it has been speculated that this explains the frequency of cohesive failure within a GIC (Tanumiharja M et al., 2000). Cohesive failure was more evident in HA-added experimental groups, and more in the Exp. 2 group than in the Exp. 1 group, as a result of increased bonding strength.

The reason why the samples were kept in the SBF fluid was to induce the formation of bone-like apatite between the interfaces of the tooth and the material, and as a result observed under SEM after 4 days, the control group revealed to have a greater porosity compared to the HA-added experimental groups. There were observable bone-like apatite particles formed on the surfaces, in the HA-added experimental groups. This is reported to be contributed by the ion exchange between the SBF and the HA soaring from the material (Santos C et al., 2001). We could observe a greater number of bone-like apatite particles in the Exp. 2 group compared to the Exp. 1 group, and their dentinal tubules were hence narrowed by the formation of these particles. There are two possible reasons that can explain why a greater number of bone-like apatite particles were formed as the size of HA particles decreased. The first reason is that because the solubility of the nano HA is greater, the particles can more actively participate in the ion exchange with the SBF fluid (Domigo C et al., 2001), and the second reason is because the nano HA has a strong adhesion strength and because it is similar to

tooth components. As it was mentioned as the reason for increased bonding strength, the strong adhesion strength and the similarity to tooth components facilitate its infiltration into the micropores of the tooth surface and the subsided nano HA particles facilitate additional particles to subside.

V. Conclusion

This study was conducted to evaluate the effect of incorporated nano HA on the demineralization resistance and bonding strength of light-cured glass ionomer cement in comparison with micro HA. The depth of cure, sensitivity to ambient light, and flexural strength, which are the necessary requirements for dental water-based light activated cements, were determined according to ISO 9917-2:1998. And in order to observe the demineralization resistant effect of each material, sectioned specimens were observed under CLSM and SEM after 4 days of demineralization. Four weeks after the assembly of tooth-cement had been immersed in SBF at 37°C, the shear bonding strength was measured and the fractured surface of the specimen was observed under SEM. According to the results, the following conclusions could be obtained.

1. The depth of cure was found to be in the decreasing order of the control, Exp. 1, and Exp. 2 group, and there were statistically significant differences between the three groups ($p < 0.05$). The curing depth in all groups satisfied the ISO 9917-2:1998 requirement for the minimum curing depth of 1 mm.
2. Regarding the sensitivity to ambient light, there were no detectable changes in the homogeneity in any group.
3. The flexural strength was found to be in the increasing order of the Exp. 2,

control, and Exp. 1 group, and there were statistically significant differences between the three groups ($p < 0.05$). All groups satisfied the ISO 9917-2:1998 requirement for the minimum flexural strength of 20 MPa.

4. Observing under the CLSM after 4 days of acid demineralization, the control group showed thicker enamel demineralization layer than in the experimental groups, and the Exp. 2 group showed the thinnest demineralization layer.
5. In SEM analysis, there was greater enamel demineralization in the control group. As less demineralized occurred under the influence of HA particles, the experimental groups revealed relatively even surface particles. Comparing the two experimental groups, the Exp. 2 group was more resistant to demineralization than the Exp. 1 group.
6. The bonding strength was found to be in the increasing order of the control, Exp. 1, and Exp. 2 group, and there were statistically significant differences between the three groups ($p < 0.05$).
7. Observing the fractured surfaces under SEM after the bonding strength test was performed, the cohesive failure ratio was found to be in the increasing order of the control, Exp. 1, and Exp. 2 group. There were bone-like apatite particles formed in the HA-added experimental groups, and a greater number of bone-like apatite particles were formed in the Exp. 2 group than in the Exp. 1 group.

15% micro HA and 15% nano HA were used in this study, and we found that although the addition of nano HA to LC GIC led to superior demineralization resistance as well as superior bonding strength, in spite of inferior flexural strength compared to the addition of micro HA. Assuming that similar results can be achieved in the oral environment, the results of this study indicates that demineralization of enamel surface can be prevented by using nano HA. Further study is needed to determine the optimal concentration of nano HA particles in LC GIC to achieve proper physical properties of the cement. In addition, the mechanism of increased demineralization resistance of LC GIC incorporated with nano HA should also be investigated.

References

Akinmade AO and Nicholson JW : Glass-ionomer cements as adhesive. Part I: Fundamental aspects and their clinical relevance. *J. Mater. Sci. Mater. Med.* 4: 93-101, 1993.

Alkinmade A : Adhesion of glass-polyalkenoate cement to collagen . *J. Dent. Research* 73, 633, 1994.

Anderson P, Bollet-Quivogne FR, Dowker SE, and Elliott JC : Demineralization in enamel and hydroxyapatite aggregates at increasing ionic strength. *Arch. Oral Biol.* 49(3): 199-207, 2004.

Arcis RW, Lopez-Macipe A, Toledano M, Osorio E, Rodriguez-Clemente R, Mutra J, Fanovich MA, and Pascual CD : Mechanical properties of visible light-cured resins reinforced with hydroxyapatite for dental restoration. *Dent. Mater.* 18: 49-57, 2002.

Bullard RH, Leinfelder KF, and Russell CM : Effect of coefficient of thermal expansion on microleakage. *J. Am. Dent. Assoc.* 116: 871-874, 1998.

Costa CAS, Giro EM, Nascimento ABL, Teixeira HM, Hebling J : Short-term evaluation of the pulpo-dentin complex response to a resin-modified glass-ionomer cement and a bonding agent applied in deep cavities. *Dent. Mater.* 19: 739-746, 2003.

Cho E, Kopel H, White SN : Moisture susceptibility of resin-modified glass-ionomer materials. *Quint. Int.* 26: 351-358, 1995.

Domingo C, Arcis RW, Lopez-Macipe A, Osorio R, Rodriguez-Clemente R, Mutra J, Fanovich MA, and Toledano M : Dental composite reinforced with hydroxyapatite: Mechanical behavior and absorption/elution characteristics. *J. Biomed. Mater. Res.* 56(2): 297-305, 2001.

Erickson RL and Glasspoole EA : Bonding to tooth structure: a comparison of glass-ionomer and composite-resin systems. *J. Esthet. Dent.* 6: 227-244, 1994.

Gao W and Smales RJ : Fluoride release/uptake of conventional and resin-modified glass ionomers, and compomers. *J. Dent.* 29: 301-306, 2001.

Geiger SB and Weiner S : Fluoride carbonatoapatite in the intermediate layer between glass ionomer and dentin. *Dent. Mater.* 9:33-36, 1993.

Gladys S, Van Meerbeek B, Braem M, Lambrechts P, Vanherle G : Comparative physico-mechanical characterization of new hybrid restorative materials with conventional glass-ionomer and resin composite restorative materials. *J. Dent. Res.* 76: 883-894, 1997.

Glasspoole EA, Ericson RL, Davidson CL : Effect of surface treatments on the bond strength of glass ionomers to enamel. *Dent. Mater.* 18: 454-462, 2002.

Griffith AA : The phenomena of rupture and flow in solids. *Philos. Trans. R. Soc. London A* 221:163-198, 1920.

Gu YW, Yap AUJ, Cheang P, and Khor KA : Effect of incorporation of HA/ZrO₂ into glass ionomer cement (GIC). *Biomaterials* 26: 713-720, 2005.

Huang M, Feng J, Wang J, Zhang X, Li Y, and Yan Y : Synthesis and characterization of nano-HA/PA66 composites. *J. Mater. Sci. Mater. Med.* 14(7): 655-660, 2003.

Itthagarun A, King NM, Yiu C, and Dawes C : The effect of chewing gums containing calcium phosphates on the remineralization of artificial caries-like lesions in situ. *Caries Res.* 39(3); 251-254, 2005.

Jeong SH, Jang SO, Kim KN, Kwon HK, Park YD, Kim BI : Remineralization potential of new toothpaste containing nano-hydroxyapatite. *Key Eng. Mater.* 309-311: 537-540, 2006.

Kim BI, Jeong SH, Jang SO, Kim KN, Kwon HK, Park TD : Tooth whitening effect of toothpastes containing nano-hydroxyapatite. *Key Eng. Mater.* 309-311, 541-544, 2006.

Kuilong LV, Jiuxing Zhang, Xiangcai Meng, Xingyi Li : Remineralization effect of the nano-HA toothpaste on artificial caries. *Key Eng. Mater.* 330-332: 267-270, 2007.

Kloke A, Tadic D, Kahl-Nieke B, Epple M : An optimized synthetic substrate for orthodontic bond strength testing. *Dent. Mater.* 13(4): 773-778, 2003.

Leyhausen G, Abtahi M, Karbakhsch M, Sapotnick A, and Geurtsen W : Biocompatibility of various light-curing and one conventional glass-ionomer cement. *Biomaterials* 19: 559-564, 1998.

Lowenstam HA, Weiner S : On biomineralization. Oxford: *Oxford University Press*, 1989.

Lucas ME : Flexural strength of hydroxyapatite-added glass ionomer cement. *J. Dent. Res.* 81: 36, 2002.

Lucas ME, Kenji Arita, and Mizuho Nishino : Toughness, bonding and fluoride-release properties of hydroxyapatite-added glass ionomer cement. *Biomaterials* 24: 3787-3794, 2003.

Mazzaoui SA, Burrow MF, Tyas MJ, Dashper SG, Eakins D, and Reynolds EC : Incorporation of Casein phosphopeptide-amorphous calcium phosphate into a glass-ionomer cement. *J. Dent. Res.* 82(11): 914-918, 2003.

Mckinney IE : Wear and microhardness of the experimental dental composites. *J. Dent. Res.* 66: 1134-1139, 1986.

Mount GJ : Glass ionomers: a review of their current status. *Oper. Dent.* 24: 115-124, 1999.

Ngo H, Mount GJ, and Peters MCRB : A study of glass-ionomer cements and its interface with enamel and dentin using a low temperature, high resolution scanning electron microscope technique. *Quintessence Int.* 28: 63-69, 1997.

Santos C, Luklonska ZB, Clatke RL, Davy KWM : Hydroxyapatite as a filler for dental composite materials: mechanical properties and in vitro bioactivity of composites. *J. Mater. Scien.* 12: 565-573, 2001.

Sennou HE, Lebugle AA, Gregorie GL : X-ray photoelectron spectroscopy study of the dentin-glass ionomer cement interface. *Dent. Mater.* 15: 229-237, 1999.

Tanumiharja M, Burrow MF, Ttas MJ : Microtensile bond strengths of glass ionomer (polyalkenoate) cements to dentine using four conditioners. *J. Dent.* 28: 361-366, 2000.

Yoon SI, Lee YK, Kim YU, Kim MC, Kim KN, Kim SO, and Choi HJ : The effects of hydroxyapatite on bonding strength between dental luting cement and human teeth. *Key Eng. Mater.* 284-286: 953-956, 2005.

국문요약

광중합형 글라스아이오노머 시멘트의 탈회 저항성과 결합 강도에 대한 나노미터 입자의 하이드록시아파타이트의 효과

연세대학교 대학원 치의학과

김 지 희

지도교수 : 최형준

광중합형 글라스아이오노머 시멘트는 불소 방출 및 상아질과 유사한 열팽창계수와 탄성계수, 법랑질과 상아질에 대한 화학적 결합, 생체친화성, 상대적으로 쉬운 사용 등의 전통적인 글라스아이오노머의 장점 뿐만 아니라 빠른 경화속도와 탈수에 대한 저항성 등의 장점을 지니고 있어 현재 많이 이용되고 있다. 그러나 다른 재료들에 비해 낮은 물리적 성질과 수분 민감성의 단점을 가지고 있어 수복물 주변의 미세누출과 하방 치아조직에 이차적인 치아 우식증이 발생하는 문제를 가지고 있기 때문에 이러한 글라스아이오노머의 단점을 극복하기 위한 여러 시도가 행해지고 있다.

하이드록시아파타이트는 생물학적 아파타이트로서 치아 법랑질과 골조직의 주요 구성 성분이고 생체 조직과의 유사성으로 인하여 치의학 분야에서는 골대체제나

치아 수복재료 등으로 사용하기 위하여 많은 연구가 진행되고 있으며 탈회된 치아 표면을 재광화 시키기 위하여 활용되고 있다.

최근 치의학 분야에서 나노기술을 치과재료에 적용시키는 연구들이 행해지고 있는데 나노미터 입자의 하이드록시아파타이트는 마이크로미터 입자에 비해 크기가 작고 표면적이 크며 용해도가 높으므로 탈회된 법랑질 표면의 미세공극을 채우고 칼슘과 인 등의 무기질 이온을 공급하는데 보다 뛰어난 효과를 보일 것으로 기대된다.

이번 연구의 목적은 광중합형 글라스아이오노머 시멘트에 마이크로 입자의 하이드록시아파타이트와 나노미터 입자의 하이드록시아파타이트를 첨가하였을 때 물리적 성질과 탈회 저항, 결합 강도의 차이를 비교하기 위함이다.

실험에 사용된 광중합형 글라스아이오노머 시멘트는 Fuji II LC (GC Co., Japan)였고 순수한 Fuji II LC GIC 는 대조군으로, 15% micro HA- Fuji II LC GIC 는 실험군 1, 15% nano HA- Fuji II LC GIC 는 실험군 2 로 설정하였다.

먼저 ISO 9917-2:1998 규정에 따라서 치과용 수성 광중합형 시멘트가 가져야 하는 기본적 성질인 중합 깊이, 주변광에 대한 민감도, 굽힘 강도에 대한 실험을 시행하였고, 탈회 저항성을 알아보기 위하여 4 일간 탈회시킨 시편을 절단하여 confocal laser scanning microscope (CLSM)와 scanning electron microscope (SEM)를 사용하여 재료 인접부 법랑질의 탈회 양상을 관찰하였다.

결합 강도 측정을 위해 재료를 치아에 부착하여 37℃의 유사체액 (simulated body fluid, SBF)에 4 주간 보관한 후 전단 결합 강도를 측정하였고 재료가 떨어져 나간 치아의 표면 상태를 알아보기 위해 SEM 을 이용하여 파절면을 관찰하였으며 실험 결과 다음과 같은 결론을 얻었다.

1. 중합 깊이는 대조군, 실험군 1, 실험군 2 순으로 감소하였으며, 세 군간에 통계학적 유의성이 있었고 ($p < 0.05$), 모든 그룹이 ISO 9917-2:1998 규정에 있는 중합 깊이의 조건을 만족시켰다. (최소 중합 깊이 = 1 mm)
2. 모든 군에서 주변광에 대한 민감도가 관찰되지 않았고, 그 균질성에 변화가 없었다.
3. 굴곡 강도는 실험군 2, 대조군, 실험군 1 순으로 증가했고, 세 군간에 통계학적 유의성이 있었다 ($p < 0.05$). 또한 모든 그룹이 ISO 9917-2:1998 규정에 있는 굴곡 강도의 조건을 만족시켰다. (최소 굴곡 강도 = 20 MPa)
4. 탈회 저항성 실험 결과 대조군 보다 실험군에서 법랑질의 탈회가 덜 발생하였고, 실험군 1 보다 실험군 2에서 법랑질의 탈회가 적게 관찰되었다.
5. SEM을 이용한 탈회면 관찰시 대조군에서 법랑질의 탈회가 더 많이 일어났고, 실험군은 하이드록시아파타이트의 영향으로 탈회가 덜 일어나 표면입자가 보다 규칙적이었다. 두 실험군을 비교했을 때 실험군 2가 실험군 1 보다 탈회에 저항하였다.
6. 결합 강도는 대조군, 실험군 1, 실험군 2 순으로 증가했으며 세 군간에

통계학적으로 유의할 만한 차이가 있었다 ($p < 0.05$).

7. SEM 상에서 결합 강도 측정 후 파절된 면을 관찰한 결과 대조군, 실험군 1, 실험군 2 순으로 응집파괴 (cohesive failure) 비율이 더 커졌다. 하이드록시아파타이트를 포함하는 실험군에서는 골 유사 아파타이트 추정 입자가 관찰되었으며 실험군 1 보다 실험군 2에서 더 많은 입자가 형성되었다.

이번 연구에서 15% micro HA와 15% nano HA를 사용했는데, nano 입자인 경우가 micro 입자의 경우 보다 굴곡 강도는 낮지만, 탈회저항성과 결합 강도가 더 우수한 것으로 나타났다. 따라서 물리적 성질의 개선을 위해서 nano HA 의 첨가 비율을 조정하는 연구가 추가로 필요할 것으로 사료된다.

핵심되는 말 : 광중합형 글라스이오노머 시멘트, 나노미터 하이드록시아파타이트,

탈회 저항성, 결합 강도